

Electronic Supplementary Information

Selective Cancer Treatment via Photodynamic Sensitization of Hypoxia-Responsive Drug Delivery

Hua He^{a,#}, Rongying Zhu^{b,#}, Wei Sun^{c,}, Kaimin Cai^d, Yongbing Chen^{b,*}, Lichen Yin^{a,*}*

^a Jiangsu Key Laboratory for Carbon-Based Functional Materials and Devices, Institute of Functional Nano & Soft Materials (FUNSOM), Collaborative Innovation Center of Suzhou Nano Science & Technology, Soochow University, Suzhou 215123, P.R. China

^b Department of Cardiothoracic Surgery, the Second Affiliated Hospital of Soochow University, Suzhou 215004, P.R. China

^c Department of General Surgery, Affiliated Shengjing Hospital, China Medical University, Shenyang 110004, China

^d Department of Materials Science and Engineering, University of Illinois at Urbana-Champaign, Urbana IL 61801, USA

[#] These authors contributed equally.

*Corresponding author:

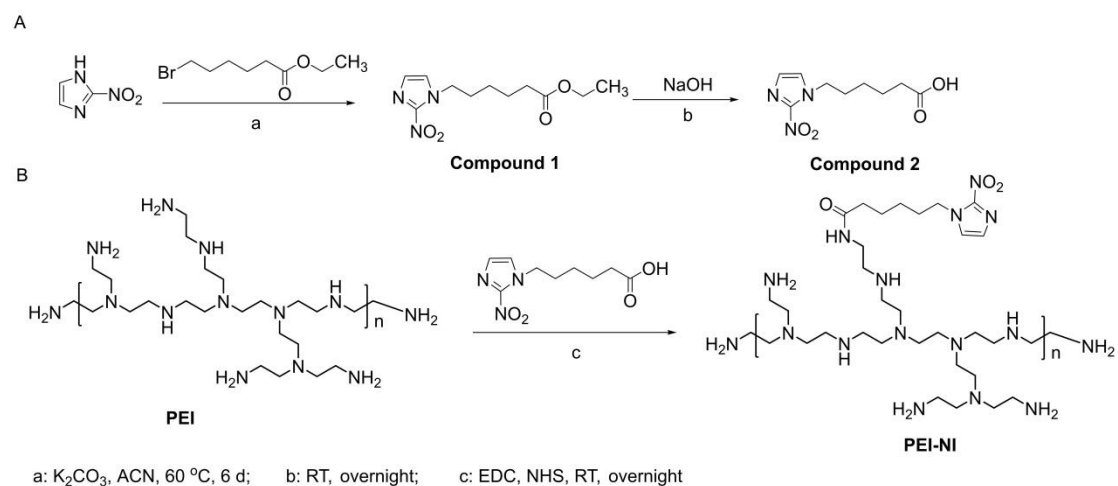
Email: lcyin@suda.edu.cn (L. Yin); Phone: 86-512-65882039;

chentongt@sina.com (Y. Chen); Phone: 86-512-67784776;

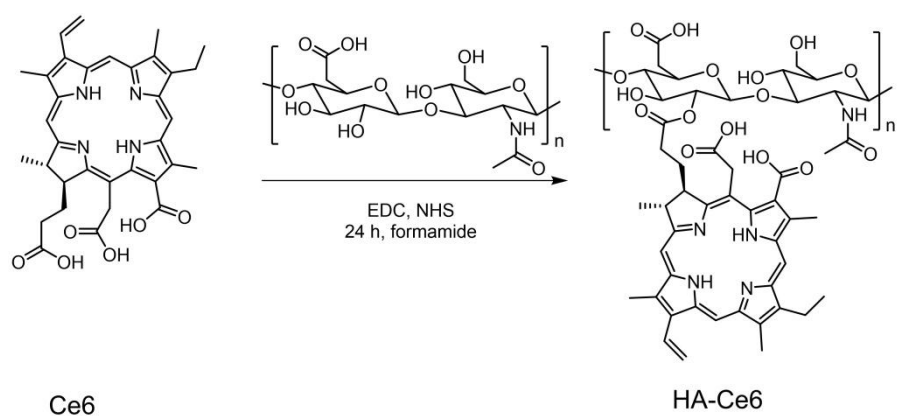
sunw@sj-hospital.org (W. Sun); Phone: 86-24-96615-31311.

Table S1 The IC₅₀ (μg/mL) of DOX in HC/PN/DOX NPs toward LLC cells with or without pre-treatment of HA.

	w/o HA	w/ HA
IC ₅₀ (μg/mL)	1.15	4.40



Scheme S1 Synthetic route of **compound 2** (A) and PEI-NI (B).



Scheme S2 Synthetic route of HA-Ce6 (HC).

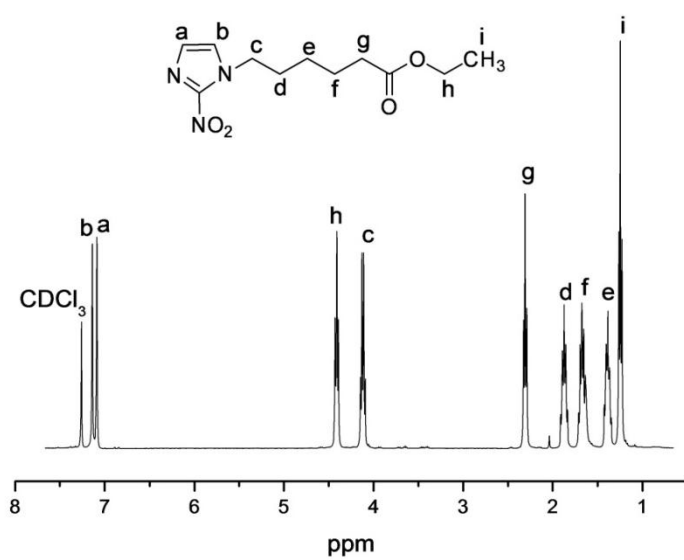


Fig. S1 ¹H NMR spectrum of **compound 1** (CDCl₃, 400 MHz).

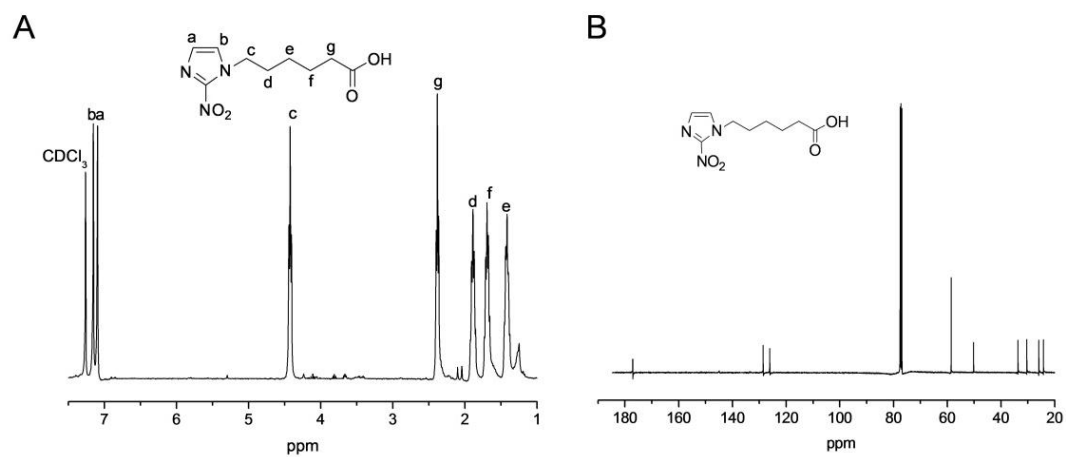


Fig. S2 ^1H NMR (A) and ^{13}C NMR (B) spectra of **compound 2** (CDCl_3 , 400 MHz).

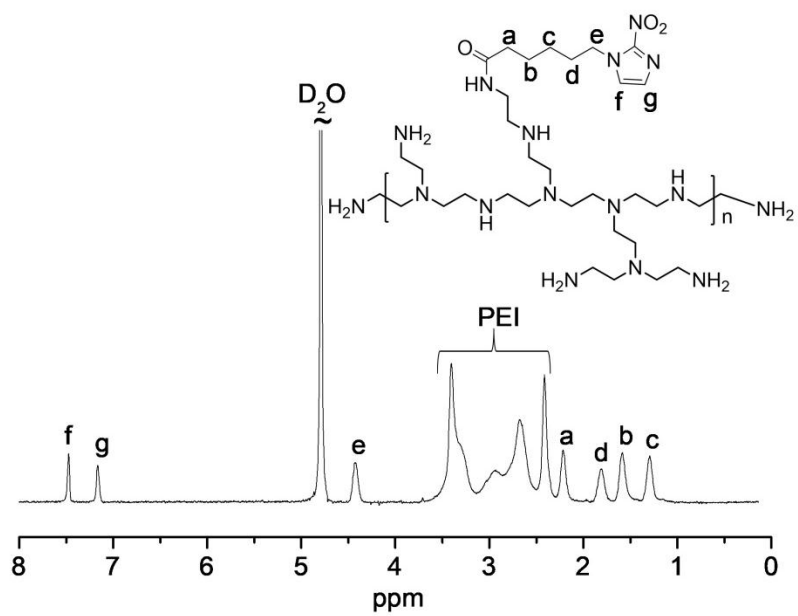


Fig. S3 ^1H NMR spectrum of PEI-NI (D_2O , 400 MHz).

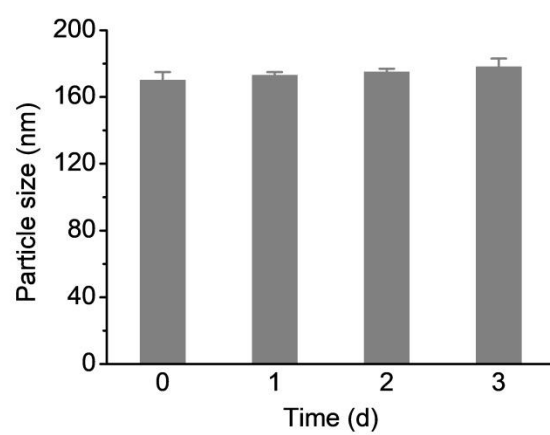


Fig. S4 Alteration of particle size of HC/PN/DOX NPs after incubation with DMEM containing 10% FBS.

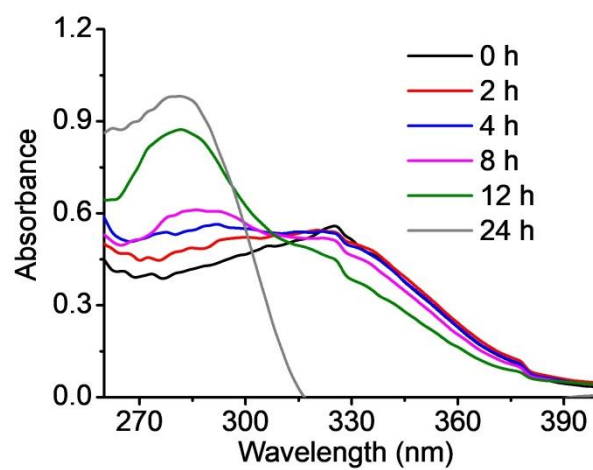


Fig. S5 UV-Vis spectra of HA/PN NPs in HEPES buffer containing 100 μ M NADPH under hypoxic condition for different time.

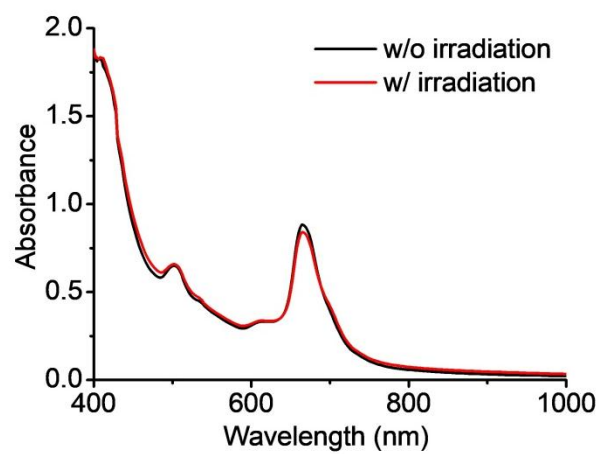


Fig. S6. UV-Vis spectra of Ce6 in HC/PN NPs before and after light irradiation (660 nm, 10 mW/cm², 30 min).

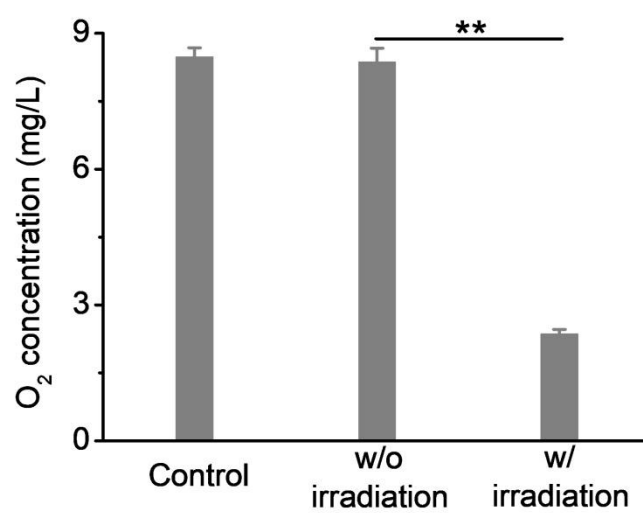


Fig. S7. Alteration of O₂ concentration in HC/PN NPs before and after light irradiation (660 nm, 10 mW/cm², 30 min).

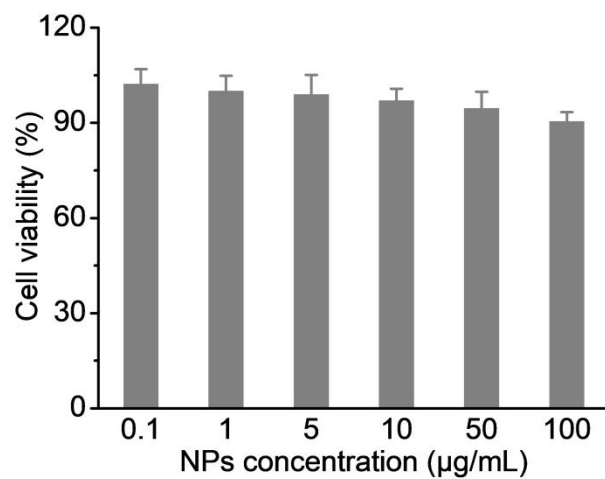


Fig. S8 Cytotoxicity of HC/PN NPs toward LLC cells following 72-h incubation at various NPs concentrations as determined by the MTT assay (n = 3).

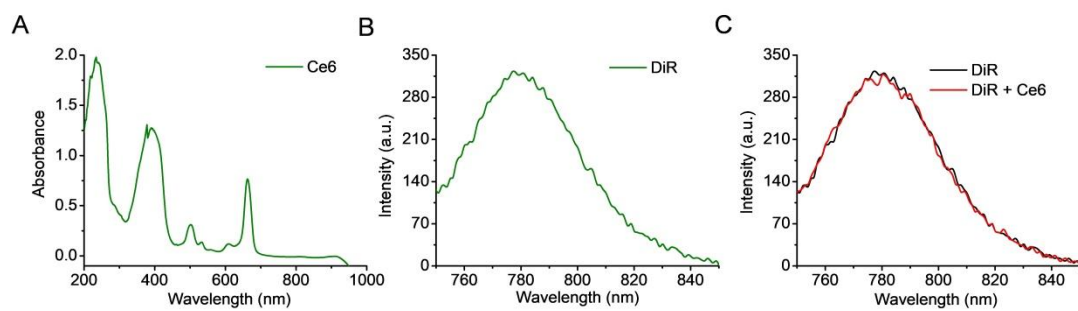


Fig. S9. (A) UV-Vis spectra of Ce6 in DMF. (B) Fluorescence spectra of DiR in DMF. (C) Fluorescence spectra of DiR and a mixture of DiR and Ce6.

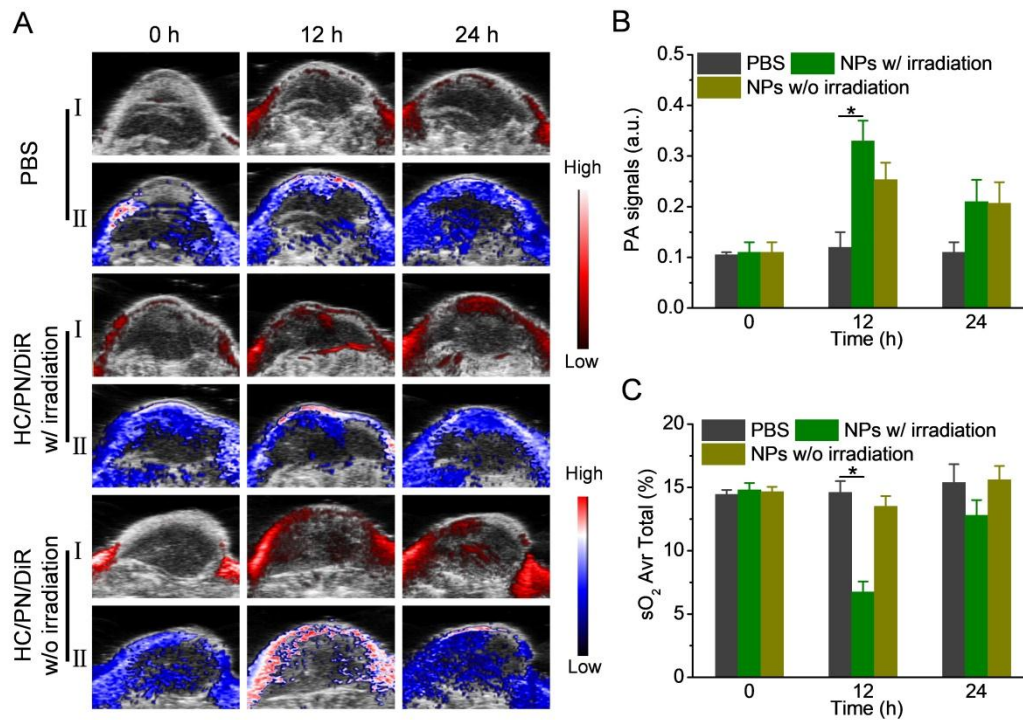


Fig. S10. (A) Representative PA images of LLC tumors showing the tumoral accumulation of DiR-containing NPs and tumoral oxygenation status as indicated by the ratios of oxygenated hemoglobin ($\lambda = 850$ nm) to deoxygenated hemoglobin ($\lambda = 750$ nm) after indicated treatments. (I: DiR; II: oxyhemoglobin). (B) Tumoral distribution level of DiR-containing NPs as indicated by the quantified PA signals in the tumors at different time points after treatment ($n = 3$). (C) Quantification of the oxyhemoglobin saturation in the tumors at different time points after treatment ($n = 3$).

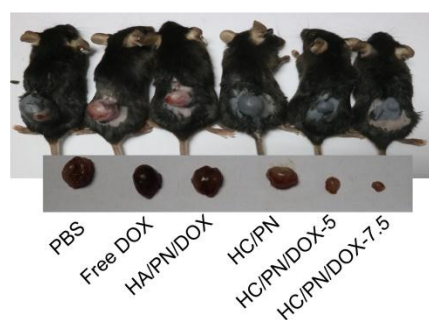


Fig. S11 *In vivo* anticancer performance of PBS, free DOX, HA/PN/DOX NPs, HC/PN NPs, and HC/PN/DOX NPs in LLC tumor-bearing C57BL/6 mice. Mice were treated as described in Fig. 6, and photographs were taken on day 12.

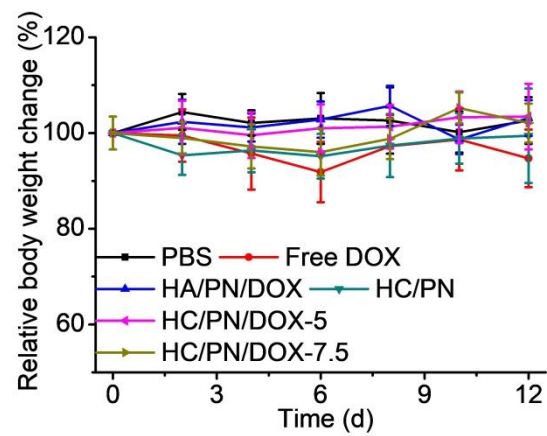


Fig. S12 Body weight changes of mice treated as described in Fig. 6 within the observation period of 12 d (n = 8).

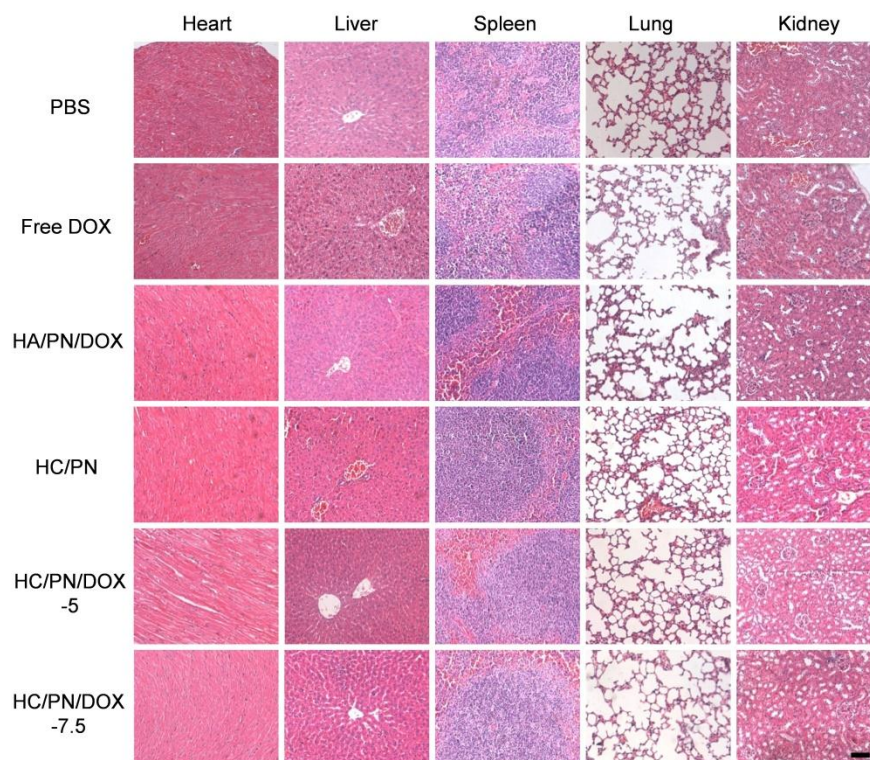


Fig. S13 H&E staining of major organ sections harvested from mice on day 12. Bar represents 100 μm .